

YALE PEABODY MUSEUM

P.O. BOX 208118 | NEW HAVEN CT 06520-8118 USA | PEABODY.YALE. EDU

JOURNAL OF MARINE RESEARCH

The *Journal of Marine Research*, one of the oldest journals in American marine science, published important peer-reviewed original research on a broad array of topics in physical, biological, and chemical oceanography vital to the academic oceanographic community in the long and rich tradition of the Sears Foundation for Marine Research at Yale University.

An archive of all issues from 1937 to 2021 (Volume 1–79) are available through EliScholar, a digital platform for scholarly publishing provided by Yale University Library at <https://elischolar.library.yale.edu/>.

Requests for permission to clear rights for use of this content should be directed to the authors, their estates, or other representatives. The *Journal of Marine Research* has no contact information beyond the affiliations listed in the published articles. We ask that you provide attribution to the *Journal of Marine Research*.

Yale University provides access to these materials for educational and research purposes only. Copyright or other proprietary rights to content contained in this document may be held by individuals or entities other than, or in addition to, Yale University. You are solely responsible for determining the ownership of the copyright, and for obtaining permission for your intended use. Yale University makes no warranty that your distribution, reproduction, or other use of these materials will not infringe the rights of third parties.



This work is licensed under a Creative Commons Attribution-NonCommercial-ShareAlike 4.0 International License.
<https://creativecommons.org/licenses/by-nc-sa/4.0/>



Nitrification and oxygen consumption in northwest Atlantic deep-sea sediments

by John P. Christensen¹ and Gilbert T. Rowe²

ABSTRACT

The importance of nitrification in the oxygen consumption by deep-sea sediments was investigated by modelling pore water nitrate profiles from 6 northwest Atlantic cores. Total nitrification and denitrification rates were calculated from the thickness of the nitrification layer, the nitrification rate at the sediment surface (N), the coefficient of exponential decrease of the nitrification rate (B), and the first-order rate constant for denitrification. The four unknowns were determined by best fit of the model to the nitrate profiles. The nitrate profile from the furthest offshore station indicated no denitrification, so that only N and B were determined. Nitrification rates ranged from 150×10^{-6} to 3.86×10^{-6} nmole NH_4^+ $\text{cm}^{-2} \text{s}^{-1}$ at the 1850 m and the 5105 m stations, respectively. As the oxygen consumption by nitrification could account for 35% of the published total oxygen consumption at these stations, nitrification represented a significant aerobic reaction in these deep-sea sediments. Ammonium sources included an upward ammonium flux from deeper anaerobic strata (6%) and aerobic respiration of organic matter (56%) with the remainder presumably supplied by anaerobic respiration within the oxygenated strata (38%). Nitrogen budgets based on sediment traps indicated that nitrification and burial rates agreed within a factor of 2 of sediment trap organic nitrogen fluxes. Also, 70% of the nitrogen that was nitrified or buried was returned as nitrate to the water column.

1. Introduction

Chemoautotrophic microorganisms oxidize reduced inorganic compounds such as H_2S , NH_4^+ , Fe^{+2} , or Mn^{+2} to obtain energy and fix CO_2 into organic matter. Among these, nitrifiers consume oxygen to sequentially oxidize ammonium to nitrite and then to nitrate which produces elevated nitrate concentrations in both shallow-water and deep-sea sediments (Vanderborght and Billen, 1975; Jahnke *et al.*, 1982; Goloway and Bender, 1982). Although this process is important in stimulating sedimentary denitrification, its role in oxygen consumption by deep-sea sediments is uncertain. It has been assumed to approximate the stoichiometry of 16 ammoniums nitrified per 138 oxygen molecules consumed in total such that nitrification accounts for 23% of the oxygen consumption rate (Richards, 1965; Bender *et al.*, 1977). This ratio has been experimentally verified in sediments from the central equatorial Pacific (Grundmanis and

1. Bigelow Laboratory for Ocean Sciences, West Boothbay Harbor, Maine, 04575, U.S.A.

2. Brookhaven National Laboratory, Upton, New York, 11973, U.S.A.

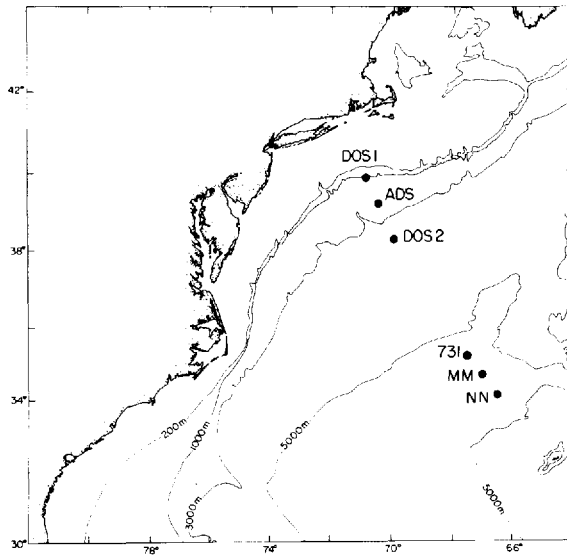


Figure 1. Station locations.

Murray, 1982), but a greater role of nitrification in some sediments has been postulated (Rowe, 1981). More recently, nitrification was shown to account for 35% of the oxygen consumption in shallow coastal sediments (Seitzinger *et al.*, 1984). In this report, we estimate the nitrification rates in continental slope and abyssal plain sediments in the northwest Atlantic Ocean based on analytical models of interstitial-water nitrate profiles and compare them with previously published oxygen consumption rates measured at these same locations.

2. Methods

Six gravity cores were collected in June 1981 on the R/V *Oceanus* cruise number 100 from water depths ranging from 1850 to 5120 m in the northwestern Atlantic Ocean (Fig. 1). Immediately upon retrieval of the cores, pore water was separated from the sediment particles by centrifugation of the whole sediments at 12,000 g (15 min) and then filtered through 0.4 μm Nucleopore® filters. Aliquots were separated for the determination of manganese, ammonium, nitrite, and nitrate concentrations. In order to minimize bacterial alteration of the nitrogen concentrations during the 2–4 hr processing, 1% v:v of concentrated HgCl_2 was added to each nitrogen aliquot. Soluble manganese was determined by the method of Armstrong *et al.* (1979) within 2 hr of core retrieval. Ammonium and nitrate were measured by the methods of Strickland and Parsons (1972). Nitrate was then measured by the method of Gardner *et al.* (1976), and values of about 0.5 μM were indistinguishable from background.

3. Results

At all 6 stations, nitrate profiles had subsurface nitrate concentrations greater than that in the bottom water ($18 \mu\text{M}$), indicating nitrate production by nitrification (Table 1, Fig. 2). At station NN, nitrate concentrations asymptotically approached concentrations of $32 \mu\text{M}$ at 30 cm suggesting nitrification occurred throughout the core. At the other 5 stations, a subsurface maximum occurred indicating strata with nitrification overlying a zone of denitrification. At 3 of these stations (DOS1, ADS, and DOS2), nitrate was depleted to background levels within the core, and at station MM nitrate probably would have disappeared within a few centimeters of the deepest sampled depth since nitrate at this depth had been reduced to $1.6 \mu\text{M}$. Nitrate disappeared at progressively deeper horizons with increasing water-column depth and distance offshore. At station DOS1 (1850 m), the nitrate disappeared at about 4 cm, at station ADS it was about 10 cm, at station DOS2 it was about 8 cm while at station MM it was about 60 cm.

The distributions of nitrite, ammonium, and manganese in the interstitial waters were related to the distribution of nitrate. Nitrite profiles had a subsurface maximum (up to $2.3 \mu\text{M}$) just above the nitrate disappearance depth. Although nitrite maxima have not been observed in *in situ* separated pore water samples, these maxima are frequently seen in cores and apparently are associated with denitrification (Emerson *et al.*, 1980). In association with nitrate exhaustion, ammonium and dissolved manganese concentrations increased greatly. Contrary to our data, previous *in situ* measurements of a nitrate flux into the sediments of station ADS suggested that continuously decreasing nitrate profiles should have been observed (Smith *et al.*, 1978). However, our data agree well with one nitrate profile measured at a site between stations ADS and DOS2 (Hinga *et al.*, 1979) suggesting that our data are accurate.

4. Discussion

The distribution of biochemical reactions in sediments is related to the thermodynamic favorability of the reactions (Froelich *et al.*, 1979). Thus, oxygen consumption proceeds until oxygen concentrations reach sufficiently low levels (about $3 \mu\text{M}$, Devol, 1978) whereupon nitrate reduction and denitrification become energetically favorable. During denitrification, nitrite concentrations can be elevated. Redox conditions characteristic of denitrification also favor the stability of soluble manganese (Mn^{+2}). Following nitrate disappearance, more anaerobic processes such as iron solubilization and sulfate reduction become favorable. This scheme conforms to our data. Within the aerobic layer, nitrification proceeds as indicated by the low ammonium and elevated nitrate concentrations. Nitrite maxima occur just above the depth of nitrate disappearance and large accumulations of ammonium and manganese begin at or just below this depth.

In aerobic deep-sea sediments with plentiful oxygen, nitrate concentrations asymp-

totically approach a maximum value (Grundmanis and Murray, 1982) as seen in our station NN. In this case, the steady-state nitrate distribution has been described by the equation (Goloway and Bender, 1982),

$$0 = \phi D \frac{\partial^2 C}{\partial z^2} - \phi w \frac{\partial C}{\partial z} + \phi N \exp(-Bz) \quad (1)$$

where D is the effective diffusivity of nitrate in the pore water, C is the nitrate concentration (nmole/ml), and w is the sedimentation rate (cm/s). Depth in the sediment is z (cm), porosity is ϕ (ml cm⁻³), and $N \exp(-Bz)$ is the nitrification rate

Table 1. Porewater chemistry from northwest Atlantic cores. Station locations (latitude N and longitude W) and water column depth are given. Depth in the core (Z) is in cm and concentrations are in μM . *was not detected.

Station DOS1 Lat 39°45.1' Long 70°40.0' Depth 1840 m					Station 731 Lat 34°57.0' Long 67°7.7' Depth 5120 m				
Z	NO3	NO2	NH4	Mn	Z	NO3	NO2	NH4	Mn
0-1	30.2	.23	8.2	2.6	0-1	21.8	1.10	3.1	1.1
1-2	31.1	.41	8.1	7.6	1-2	25.1	.38	1.9	1.8
2-3	22.5	1.32	7.6	9.3	2-3	25.4	.12	1.4	1.8
3-4	9.36	1.99	3.7	10.0	3-4	28.5	.09	.02	1.1
4-5	4.00	.47	8.0	11.2	6-8	28.7	0	1.5	1.5
5-6	1.24	.44	18.6	13.4	10-12	26.4	.21	1.1	3.1
7-8.5	.68	.17	37.6	18.2	14-16	27.6	.15	1.9	1.8
10-11.5	1.09	0	58.8	21.1	19-21	25.9	0	0.7	2.2
14-15.5	.80	.17	87.7	23.3	24-26	24.2	0	—	2.4
17-18.5	—	—	121.	25.5	29-31	25.0	.09	—	0.5
20-21.5	.95	0	135.	24.2	31-33	23.5	.12	—	1.8
22.5-24	.10	0	157.	24.6					

Station ADS Lat 39°45.1' Long 70°40.0' Depth 2850 m					Station MM Lat 34°41.9' Long 66°29.3' Depth 5105 m				
Z	NO3	NO2	NH4	Mn	Z	NO3	NO2	NH4	Mn
0-1	20.6	0.02	5.7	1.1	0-1	18.7	.47	5.6	7.8
1-2	27.7	1.17	23.4	1.4	1-2	18.3	.33	4.1	7.4
2-3	19.0	.94	10.3	1.4	2-3	20.2	.05	2.7	6.3
3-4	18.6	.15	4.1	4.3	6-8	20.6	.19	2.4	8.1
4-5	14.9	.02	1.9	6.6	10-12	21.4	.28	1.7	7.5
5-6	12.5	.02	1.8	7.9	15-17	21.7	.05	8.9	11.1
7-8	5.71	2.27	3.0	9.8	22-24	18.4	.05	0.8	12.5
8-9.5	3.66	1.22	4.4	12.8	27-29	16.3	.05	0.8	12.7
14-16	.54	.30	20.5	76.5	35-37	11.9	0	1.6	12.5
20-22	.86	.28	32.5	94.3	43-45	8.53	.02	0.8	13.8
30	.96	.35	48.6	103.3	50-52	4.41	.02	1.1	13.8
40	.40	.40	60.2	104.6	55-57	1.60	.02	1.2	16.9

Table 1. (Continued)

Station DOS2 Lat 38°18. ' Long 69°33. ' Depth 3630 m					Station NN Lat 33°56.0' Long 65°51.4' Depth 5090 m				
Z	NO3	NO2	NH4	Mn	Z	NO3	NO2	NH4	Mn
0-1	24.4	.57	2.6	2.5	0-1	22.4	.58	2.7	*
1-2	23.9	.46	2.6	0	1-2	23.9	.05	1.2	*
2-3	22.8	.46	3.9	0	2-3	24.8	0	1.5	*
4-5	15.3	.69	5.0	2.8	3-4	27.9	0	1.9	*
6.5-8	4.69	1.00	2.0	4.1	7-9	28.6	.10	2.1	*
9.5-11	2.28	.23	5.3	40.1	12-14	30.4	.13	1.5	*
13-15	—	.52	14.5	60.1	17-19	32.2	.10	2.3	*
17-19	1.45	.34	21.5	62.3	22-24	31.9	.08	1.5	*
24-26	3.43	0	37.4	51.2	26-28	31.8	0	5.7	*
30-32	—	.17	46.0	45.7	30-32	31.4	.02	1.9	*
36-38	1.31	0	57.8	44.8					
41-43	0.55	.03	67.2	47.3					

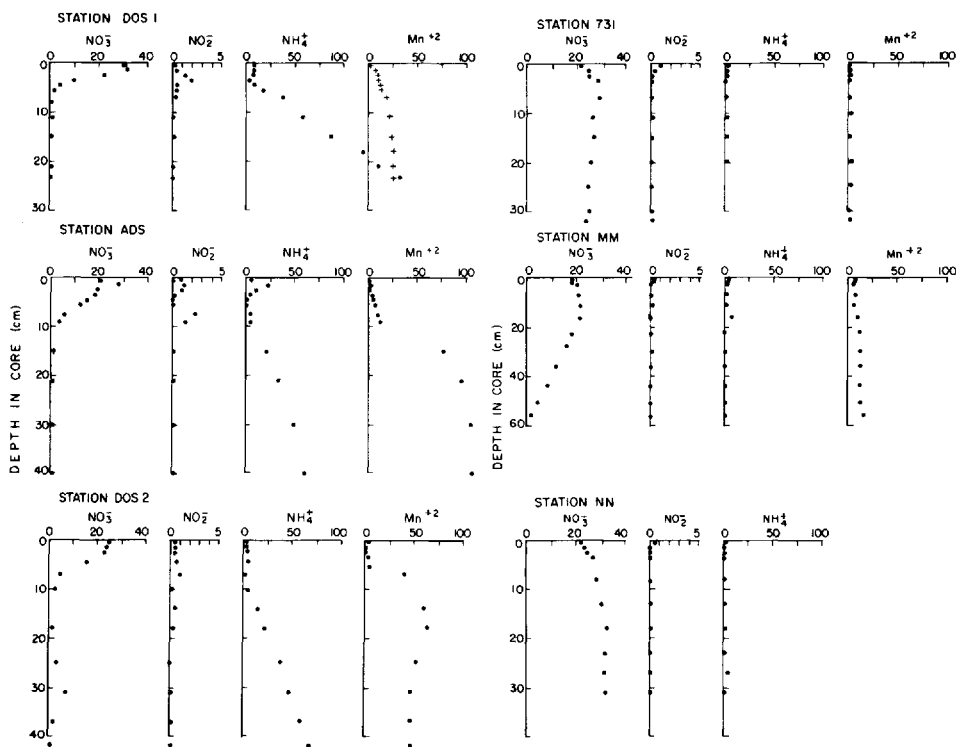


Figure 2. Porewater solute profiles in μM .

where N is the rate at the sediment surface ($\text{nmoles ml}^{-1} \text{ s}^{-1}$) and B (cm^{-1}) is the coefficient describing the exponential decrease of this rate with depth.

With the boundary conditions,

$$\begin{aligned} z = 0, \quad C &= C_0 = 18 \mu\text{M}, \\ z = \infty, \quad dC/dz &= 0, \end{aligned}$$

the solution to this equation is

$$C = C_\infty - (C_\infty - C_0) \exp(-Bz), \quad (2)$$

where C_∞ is the concentration at infinite depth. The boundary conditions require that

$$N = (C_\infty - C_0) B(DB + w). \quad (3)$$

The total nitrification rate, R_n , is

$$R_n = \int_0^\infty \phi N \exp(-Bz) dz = \phi N/B \quad (4)$$

where porosity is assumed to be a constant with depth and an average value used. When w , the sediment accumulation rate, is insignificant, this solution is identical to the nitrate flux equation derived by Goloway and Bender (1982, their Eq. 9) where their factor, $(\text{KOM}/\text{DOM})^{1/2}$, is equal to our B .

To determine the nitrification rate, Eq. 2 was fit to the nitrate data at station NN using the NLIN procedure of the SAS statistical package (Anonymous, 1979) which was run on the University of Maine's IBM 370 computer. The method varies C_∞ and B to obtain the least value of chi-square between the model-predicted nitrate profile and the measured data. Porosity was 0.7 (Christensen, 1983). The effective molecular diffusivity for nitrate was $4.2 \times 10^{-6} \text{ cm}^2/\text{s}$ (Goloway and Bender, 1982). The sedimentation rate was 5 cm/1000 yr (Ericson *et al.*, 1961). The results are given in Table 2 and plotted versus the measured nitrate profile in Figure 3. The results were altered by less than 5% even when advective vertical velocities were varied by 3 orders of magnitude (Sayles, 1981).

Nitrification coupled to denitrification. In sediments with a nitrifying zone overlying the denitrification zone, the nitrate distribution is determined by the nitrification equation (Eq. 1) in the nitrification zone of depth Z_n ($0 < z \leq Z_n$) and by the steady-state equation for denitrification in the deeper sediments ($Z_n < z < \infty$, Vanderborgh and Billen, 1975; Goloway and Bender, 1982).

$$0 = \phi D \frac{\partial^2 C}{\partial z^2} - \phi w \frac{\partial C}{\partial z} - \phi KC \quad (5)$$

where K is the first order rate constant (s^{-1}) for denitrification. The nitrification and denitrification rates can be determined by solving the coupled Eqs. 1 and 5. Unlike

Table 2. Model parameters and rates estimated from pore water nitrate profiles. The nitrification zone thickness is Z_n . The nitrification rate at the sediment surface is N and B is the coefficient of exponential decrease of this rate with depth in the core. Denitrification occurs below Z_n and the first-order denitrification rate constant is K . The difference in the depth-integrated rates of nitrification (R_n) and denitrification (R_d) is the outward surface flux of nitrate (F). In the stoichiometric model, Z_n , B , and N are determined by best fit procedures, while K is calculated from these parameters (see text). When Z_n was independently prescribed from the nitrite and manganese data, B , N , and K were determined by best fit procedures. The data from station NN were fit to the nitrification model without denitrification to determine the parameters, B and C_∞ (the asymptotic nitrate concentration, 31.31 μM). N was then calculated (see text). The chi square value of the best fits are given (CHI). At several stations, nearly identical results were obtained from repeated fits starting from different initial guesses of the unknowns which suggests convergence to a unique solution at each station.

Station	Z_n (cm)	B (cm^{-1})	N ($\frac{\text{nmole}}{\text{ml s}}$)	K (s^{-1})	R_n R_d F ($\frac{10^{-6} \text{ nmole}}{\text{cm}^2 \text{ s}}$)	CHI
Stoichiometric nitrification-denitrification model						
DOS1	2.63	0.661	1.57×10^{-4}	2.90×10^{-6}	137. 47.7 89.3	1.18
ADS	3.62	0.824	5.92×10^{-5}	2.84×10^{-7}	47.7 13.7 34.0	4.90
DOS2	4.15	0.582	4.25×10^{-5}	4.79×10^{-7}	46.6 16.0 30.6	2.94
731	9.91	0.638	2.00×10^{-5}	1.91×10^{-10}	21.8 0.55 21.3	0.847
MM	38.8	0.0358	2.63×10^{-7}	2.06×10^{-8}	3.86 2.09 1.77	0.755
Nitrification-denitrification model with independently prescribed Z_n						
DOS1	3.5	1.41	3.03×10^{-4}	5.75×10^{-6}	150. 35.6 114.	0.568
ADS	8	1.61	1.23×10^{-4}	1.83×10^{-6}	53.7 9.1 44.6	4.65
DOS2	8	1.84	1.83×10^{-4}	6.32×10^{-6}	69.7 10.3 59.4	2.24
Nitrification model						
NN	—	0.347	6.73×10^{-6}	—	13.6 — 13.6	1.51

previous models that ignored advection (Vanderborght and Billen, 1975), we retained this term. To constrain the possible solutions, parameters based on the oxygen distributions have also been incorporated (Jahnke *et al.*, 1982; Goloway and Bender, 1982), but since we wished to compare the model-estimated nitrification rates with measured oxygen consumption rates, we attempted to solve these equations independently of the oxygen distribution.

Eqs. 1 and 5 were solved simultaneously with the same boundary conditions as used previously and by requiring that concentrations be equal and continuous at the boundary depth, Z_n , i.e.

$$z = Z_n, \quad C \text{ from Eq. 1} = C \text{ from Eq. 5, and,}$$

$$z = Z_n, \quad (dC/dz) \text{ from Eq. 1} = (dC/dz) \text{ from Eq. 5.}$$

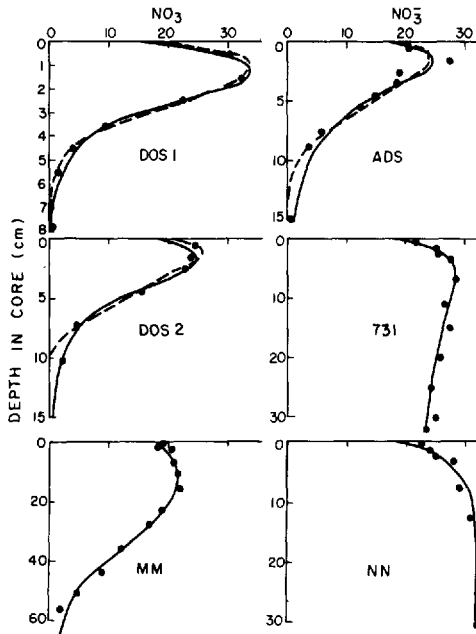


Figure 3. Nitrate data and model determined profiles for the stoichiometric model (solid line) and the independently fixed Z_n model (dashed line). Concentrations are in μM .

The solution is thus,

$$C = C_0 - \frac{D}{w} C'_0 + \frac{N}{wB} + \frac{D}{w} \left(C'_0 - \frac{N}{DB + w} \right) \exp(wz/D) - \frac{N}{B(DB + w)} \exp(-Bz) \quad (6)$$

for $0 < z \leq Z_n$, and

$$C = C_n \exp(-p(z - Z_n)) \quad (7)$$

for $Z_n < z < \infty$. The constants C'_0 (the concentration gradient at the sediment surface), p , C_n (the concentration at Z_n) are given by:

$$C'_0 = \frac{C_0 + \frac{N}{wB} - \frac{N}{DB + w} \left(\frac{D}{w} + \frac{1}{p} \right) \exp(wZ_n/D) - \frac{N}{DB + w} \left(\frac{1}{B} - \frac{1}{p} \right) \exp(-BZ_n)}{\frac{D}{w} - \left(\frac{D}{w} + \frac{1}{p} \right) \exp(wZ_n/D)} \quad (8)$$

$$p = \left(\frac{w^2}{4D^2} + \frac{K}{D} \right) - \frac{w}{2D} \quad (9)$$

$$C_n = C_0 - \frac{D}{w} C'_0 + \frac{N}{wB} + \frac{D}{w} \left(C'_0 - \frac{N}{DB + w} \right) \exp(wZ_n/D) - \frac{N}{B(DB + w)} \exp(-BZ_n) \quad (10)$$

The depth integrated nitrification and denitrification rates are

$$R_n = \phi \frac{N}{B} (1 - \exp(-BZ_n)) \quad (11)$$

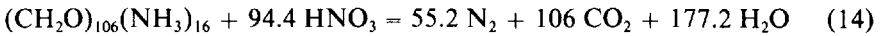
$$R_d = \phi KC_n/p. \quad (12)$$

This series of equations included 4 unknowns (N , B , Z_n , and K). In principle, these four unknowns could be determined by NLIN by varying all four simultaneously. In practice, results from these attempts were highly variable suggesting a unique solution was difficult to find perhaps because there were insufficient data within the denitrification zone to accurately define the exponentially decreasing profile predicted by Eq. 7. These equations were successfully fit to the measured data when one of the 4 unknowns was independently prescribed. The first of two approaches to prescribe these unknowns used a stoichiometric relationship of nitrification and denitrification rates at the denitrification horizon. The second used the measured profiles of nitrite and manganese to assess the anaerobic horizon.

The first approach assumed that the carbon oxidation rate was continuous across the nitrification-denitrification boundary. If oxygen respiration of organic matter was the dominant diagenetic reaction in the nitrification zone (Richards, 1965),



then nitrification is stoichiometrically linked to the carbon oxidation. Similarly, denitrification is coupled to carbon oxidation by the equation,



At Z_n , the carbon oxidation rate for both Eqs. 13 and 14 must be equal so that the nitrification rate may be related to the denitrification at this depth:

$$\phi N \exp(-BZ_n) * 106/16 = \phi KC_n * 106/94.4 \quad (15)$$

Although C_n is a complex function of K (Eq. 10), it may be simplified by recognizing that p in Eq. 9 may be approximated as,

$$p = (K/D)^{0.5} \quad (16)$$

Substituting this into Eqs. 10 and 15 and solving for K results in:

$$K = \frac{94.4^2 * (DB + w)^2 * \exp(-2BZ_n)}{16^2 * D * (\exp(wZ_n/D) - \exp(-BZ_n))^2} \quad (17)$$

Using Eq. 17 to calculate K , the profile that best fit the nitrate data was determined for the 5 stations (DOS1, ADS, DOS2, 731, and MM). The values of N , B , Z_n , K , R_n , and R_d are listed in Table 2 and plotted in Figure 3. It could be argued that possible variations in the C/N ratio of the metabolized organic material, anaerobic respiration within the aerobic zone, or oxidation of upward diffusing ammonium produced at depth could alter the exact stoichiometry in Eqs. 13 and 14 and thereby effect the model-estimated rates. To test the sensitivity of the rates to possible variations in the above stoichiometry, the ratio of 94.4/16 was doubled using data from station DOS2 which resulted in about a 5% increase in R_n and a 5% decrease in R_d . The insensitivity of R_n and R_d to variations in K can be conceptually viewed as a result of the determination of the best fit. Although the parameters required to obtain the best fit may vary, similar best-fit profiles should yield similar nitrate gradients which define the fluxes and depth-integrated rates.

An alternative to evaluating K by this stoichiometric relationship was to independently evaluate Z_n based on the nitrite and manganese data. The chosen values for Z_n were intermediate between the nitrite maximum and the inflection point of the manganese profiles (Table 1, Fig. 2). The best fit profiles for the nitrate data at stations DOS1, ADS, and DOS2 were determined by varying N , B , and K (Table 2, Fig. 3). Stations 731 and MM could not be fit with this procedure because the cores were not long enough to penetrate the denitrifying regions as evidenced by the nitrite subsurface maximum and the increasing manganese concentrations. To test for the sensitivity of the integrated rates on the selected values of Z_n , Z_n was varied by 2 cm (from 8 to 6 cm) at station DOS2. The nitrification and denitrification rates were increased by about 6% and 8% respectively, indicating that reasonable uncertainty in Z_n would not affect our results much.

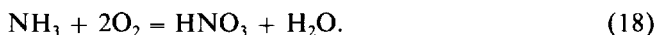
Values of the individual parameters N , B , Z_n , and K differed between the two models. Most noticeable was the shallow Z_n calculated from the stoichiometric model (Table 2). It averaged 60% of that estimated directly from the nitrite and manganese profiles at stations DOS1, ADS, and DOS2. Also, at station MM, this model yielded a very shallow Z_n of 38.8 cm, yet no other indication of anaerobiosis were observed at this depth. Thus, of the two models, the nitrite and manganese defined Z_n appear more reasonable. One consequence of the nitrite-manganese fit is that rate coefficients, N , B , and K , are much greater than in the stoichiometric model. For nitrification, a larger B means that a greater proportion of the total nitrification rate occurs near the sediment-water interface. The stoichiometric model resulted in only slightly lower nitrification rates (82% average for the three stations), but moderately higher denitrification rates (147% average) than the results when Z_n was fixed by the porewater profiles. The nitrate fluxes into the water column estimated by the stoichiometric model averaged 69% of the results of the other model for these three stations.

However, because the integrated nitrification rates calculated by the two models were not greatly dissimilar, either can be used to compare the importance of

Table 3. Comparison of oxygen consumption by nitrification with total oxygen consumption rate measured by Smith (1978) at the same stations. The total nitrification rate, R_n , is converted to an oxygen demand using a molar stoichiometry of $20_2/\text{NH}_4^+$ (Gundersen and Mountain, 1973, see text).

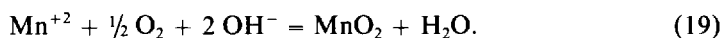
Station	Total	Stoichiometric model			Independently fixed Z_n		
	O ₂ Consumption $\mu\text{mole O}_2$ m ² hr	R_n 10^{-6} nmole cm ² s	O ₂ equiv. $\mu\text{mole O}_2$ m ² hr	% of Total	R_n 10^{-6} nmole cm ² s	O ₂ equiv. $\mu\text{mole O}_2$ m ² hr	% of Total
DOS1	22.	137.	9.9	45	150.	10.8	49
ADS	16.	47.7	3.4	21	53.7	3.9	24
DOS2	10.	46.6	3.4	34	69.7	5.0	50
MM	1.	3.86	.28	28	—	—	—
NN	3.	13.6	.98	33	—	—	—

nitrification in consuming oxygen. Oxygen consumption rates due to nitrification were estimated based on the stoichiometry (Gundersen and Mountain, 1973),



Five of our stations were located where Smith (1978) measured total oxygen consumption rates by implanting belljars on the sediments (Table 3). When our estimates of oxygen consumption by nitrification were compared with Smith's rates, nitrification accounted for 35% (range 21–50%) of the total oxygen demand. This was greater than the 23% predicted from Eq. 13. This high percentage was an unexpected result and indicated (1) that nitrification may be more significant in deep-sea oxygen consumption than previously believed and (2) that less of the oxygen consumption may be due to typical respiratory pathways. Nitrification also accounted for about 35% of the oxygen consumption in organic rich sediments in Narragansett Bay (Seitzinger *et al.*, 1984), which agreed well with our estimate even though it was a very dissimilar environment. In both environments, however, organic matter was prevalent enough that ammonium accumulated and was not limiting. In contrast, in the central Pacific, nitrate and oxygen profiles indicated that nitrification followed the stoichiometry of Eq. 13 (Grundmanis and Murray, 1982). Those sediments were highly aerobic with oxygen concentrations greater than 25% of the bottom water concentrations even at 50 cm in the sediments, suggesting that metabolism was limited by the paucity of utilizable organic material and that nitrification was limited by ammonium production via Eq. 13. Thus, the enhanced role of nitrification would not be expected in much of the deep sea where organic matter limits respiratory ammonium regeneration but would be possible in areas with sufficient organic material.

We calculated the amount of oxygen consumption that might be due to manganese oxidation based on the reaction,



This reaction accounted for no more than 3% of the total oxygen consumption (Table 4), indicating that possible autotrophy associated with this reaction may be unimportant in our study.

The importance of different sources of ammonium used in nitrification may be calculated from stoichiometric considerations. With 35% of the oxygen consumption due to ammonium oxidation and 65% due to aerobic respiration of organic matter, 17.5 moles of ammonium were nitrified for every 100 moles of oxygen consumed ($.35 \times 100 \times 1 \text{ NH}_4^+ / 2\text{O}_2$). Aerobic respiration produced 9.8 moles of ammonium ($.65 \times 100 \times 16 \text{ NH}_4^+ / 106 \text{ O}_2$) or 56% of the total. The upward flux of ammonium from the deeper anaerobic strata represented about 6% of the total nitrification rate at our shallower stations (Table 4) so that this source supplied 1.0 mole of the above total. The remaining 6.7 moles or 38% were unaccounted for but were necessary to maintain the observed nitrate profiles. Anaerobic metabolism within microenvironments in the aerobic zone probably produced this additional ammonium (Jorgensen, 1977; Wilson, 1978; Jenkins and Kemp, 1984).

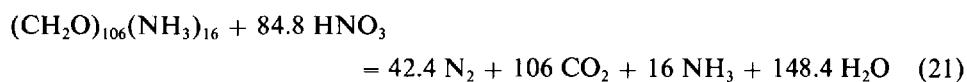
If anaerobic microzonal respiration were important within the aerobic zone, then denitrification was probably occurring within the aerobic strata. Microzonal denitrification within the aerobic sediments has not been considered in previous studies of the nitrate distribution in deep-sea sediments, yet much of the literature data may be interpreted in light of this hypothesis. Jahnke *et al.* (1982) presented 8 total inorganic nitrogen profiles from the equatorial Atlantic and Pacific which contained subsurface maxima of between 40 and 50 μM ; 6 of these maxima were less than model-predicted maxima by between 5 and 10 μM . Although those authors suggested several contributing factors to this difference, the primary factor in their view was the possible increase in the C/N ratio of the metabolizable organic material with depth in the cores. Goloway and Bender (1982) expected nitrate concentrations to follow the 16:138 $\text{NO}_3^-:\text{O}_2$ stoichiometry of our Eq. 13 but found that the ratio, $d(\text{NO}_3):d(\text{O}_2)$, was generally between 25 and 69% of that expected for both their model 2 and 3 results. They suggested that this lack in nitrate relative to oxygen could be due either to incomplete conversion of ammonium to nitrate as evidenced by measurable porewater ammonium concentrations within the aerobic zone or to C/N ratios of the metabolized organic material being greater than 106:16. In this case, higher C/N ratios would have resulted in less ammonium released during respiration and possibly would have limited the nitrification rate. We agree that this was a probable factor especially in regions with large inputs of terrigenous organics with characteristically high C/N ratios or at depth in cores where metabolism has removed the easily metabolized organic matter of low C/N ratios. However, it was equally plausible that the low total inorganic nitrogen content of Jahnke *et al.* (1982) and the low $d(\text{NO}_3):d(\text{O}_2)$ ratio of Goloway and Bender could have been due to microzonal denitrification converting some of the nitrate to N_2 which was not measured. If this microzonal denitrification was linked both to nitrate produced via nitrification and to the availability of organic material for

Table 4. The role of the deep ammonium and manganese gradients in supporting oxygen consumption. The diffusivities were 2.4×10^{-6} and 1.9×10^{-6} cm²/s for ammonium and manganese. Manganese adsorption was not considered and the flux was converted to an oxygen demand assuming 0.5 O₂ was consumed by each Mn²⁺ oxidized. These upward fluxes are apparently a small fraction of the total oxygen demand.

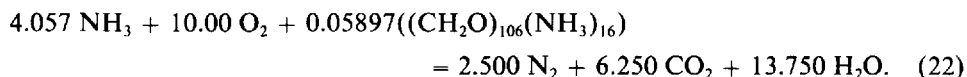
	NH ₄ ⁺ gradient nmole ml cm	NH ₄ ⁺ flux 10 ⁻⁶ nmole cm ² s	O ₂ equiv. μmole O ₂ m ² hr	% of O ₂ Demand	Mn ²⁺ gradient nmole ml cm	Mn ²⁺ flux 10 ⁻⁶ nmole cm ² s	O ₂ equiv. μmole O ₂ m ² hr	% of O ₂ Demand
DOS1	8.04	13.5	.97	4.4	2.0	2.6	.05	0.2
ADS	2.58	4.33	.31	1.9	10.2	13.4	.24	1.4
DOS2	2.15	3.61	.26	2.6	12.0	15.7	.28	2.8

respiration, then it should have been more important in cores with plentiful metabolizable organic material since this would have supplied both the required organics for the heterotrophic denitrifiers and the nitrate via ammonium oxidation by the nitrifiers (Sorensen *et al.*, 1984). Conversely, in highly aerobic sediments as in the mid-Pacific where the availability of organic material limits both oxygen consumption and ammonium availability, the lack of utilizable organics probably would have diminished the role of microzonal denitrification. There nitrification followed the 16:138 ratio (Grundmanis and Murray, 1982) as would have been expected when microzonal denitrification was insignificant.

Nitrification rates estimated by any of the diagenetic models may have been minimum estimates if denitrification was occurring in these anaerobic microenvironments. In this case, rates required for maintenance of the nitrate profile would have been supplemented by the nitrification that was directly coupled to denitrification (Jenkins and Kemp, 1984), and this latter rate would have been invisible to our model calculations. However, the stoichiometric influence of this coupling may be examined since the nitrate produced by this additional nitrification (Eq. 20) must balance the nitrate consumed by denitrification (Eq. 21).



If the sum of these two reactions consumes 10 moles of oxygen, then,



This equation indicates that for every 10 moles of oxygen consumed by directly coupled nitrification and denitrification, 5 moles of ammonium are oxidized. Of this, 19% was supplied from the organic matter consumed by denitrification and 81% was supplied from other anaerobic organic matter oxidations. Our earlier model results indicated that 35% of the oxygen consumption was due to nitrification, i.e. that 17.5 moles of ammonium were oxidized per 100 moles of O₂ consumed. For every additional 10% of the oxygen consumption which may have supported the direct coupling of the two processes, the additional oxidation of 5 moles of ammonium per 100 moles of oxygen consumed would have increased our base rate by about 30%. This process would have been more important in enhancing denitrification. For the 8 model results from the 5 stations with denitrification, denitrification consumed about 26% of the nitrified ammonium (Table 2) or 4.6 moles of nitrate for every 100 moles of oxygen consumed (17.5 × .26). For each additional 10% of the O₂ consumption supporting the direct coupling, denitrification would have been enhanced by 5 moles of NO₃ per 100 moles of oxygen consumed. The above equations assumed that the coupling was through nitrate.

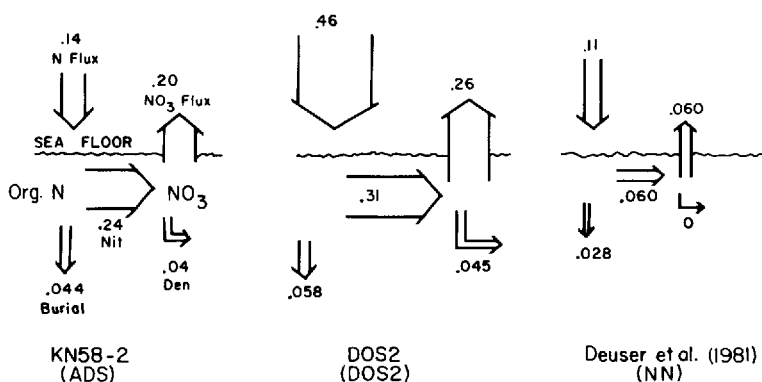


Figure 4. Flow diagrams of three deep-sea nitrogen budgets (fluxes in $\text{gm N m}^{-2} \text{yr}^{-1}$). Names of both the sediment trap stations and our stations (in parentheses) are listed. Rates of nitrification (Nit) and denitrification (Den) and nitrate fluxes (NO₃ Flux) were results of the fixed Z_n model (Table 2). Sedimenting organic nitrogen fluxes (N flux) and burial rates of left 2 stations were from Rowe and Gardner (1979). Stations KN58-2 and ADS were at the same depth but were 160 km apart. The right station represents a more pelagic (Sargasso Sea) system. Nitrogen fluxes were from Deuser *et al.* (1981) and the burial rate was calculated using an organic nitrogen content of 0.09% (Rowe and Clifford, 1978) and a sedimentation rate of 4 cm/1000 yr (Ericson *et al.*, 1961). The stations NN and that of Deuser *et al.* (1981) were 330 km apart.

If less oxidized intermediates such as nitrite or nitrous oxide were involved, then more nitrification and denitrification could have occurred per mole of oxygen consumed.

We presented Eq. 22 to examine how much the nitrification-denitrification coupling could have enhanced rates over our calculations. If this couple were important, then significant quantities of the denitrified nitrogen would have appeared to be "missing" in a typical nitrogen budget. To check this, we constructed three budgets by comparing sediment trap measurements of the organic nitrogen fluxes and nitrogen burial rates from nearby stations with our data from stations ADS, DOS2, and NN (Fig. 4). Because ammonium concentrations were low in the aerobic strata, we considered that the nitrification rates approximated ammonium regeneration rates. At station ADS, the nitrification rate exceeded the nitrogen input (nitrification was 171% of the N flux) while nitrification averaged 61% of the nitrogen input for the other two budgets. For the three budgets, the nitrification rate averaged 98% of the organic nitrogen input, and burial averaged 23% of the organic nitrogen input. Deuser *et al.* (1981) noted that short term deep-sea sediment trap fluxes may vary by several fold over the annual cycle. However, if the values were used represented true averages then the budgets were not far out of balance and the total amount of ammonium lost as N₂ was probably not extremely large. Interestingly, the nitrate flux into the water column accounted for about 70% of the sum of the nitrification and burial rates for each budget, indicating that of the sedimentary rates that we measured 30% of the nitrogen was lost by

conversion to N_2 or organic matter burial. Previous measurements of the outward ammonium flux of $0.075 \text{ gm N m}^{-2} \text{ yr}^{-1}$ at station ADS (Smith *et al.*, 1978) would have added to our budget and could have been associated with our measurable ammonium concentration at or near the sediment water interface (Fig. 2).

One consequence of autotrophic nitrification is that CO_2 is fixed into organic material. If fixation were significant, this potentially could be a source of "new" carbon for the deep-sea benthos. We estimated the importance of CO_2 fixation by assuming a stoichiometry of CO_2 fixed to ammonium oxidized of 1/10 (Billen, 1976). If 35% of the oxygen consumption is due to nitrification, then 1.75 moles of CO_2 would be fixed per 100 moles of O_2 consumed ($.35 \times 100 \times 1 \text{ NH}_3/2 \text{ O}_2 \times 1 \text{ CO}_2/10 \text{ NH}_3$). Carbon dioxide production would be the sum of aerobic and anaerobic respiration and can be calculated using the C/N stoichiometry of 106/16 and the ammonium production for aerobic and anaerobic respiration which was estimated earlier. Aerobic respiration produced 9.8 moles of ammonium/100 moles of oxygen consumed while anaerobic respiration produced 6.7 moles of ammonium/100 moles of oxygen consumed. The CO_2 production would then be 109 moles of CO_2 /100 moles of O_2 consumed. Autotrophic production by the nitrifiers then represents 1.6% of the CO_2 produced by both aerobic and anaerobic metabolism. Consequently, the "new" carbon would be of little significance in the overall carbon budget of deep-sea sediments although it may be a good source of utilizable organic matter for heterotrophic consumers.

Acknowledgments. This research was funded by National Science Foundation grants OCE-8214796 and OCE ISP-8011448 to J.P.C. This manuscript is contribution 83016 from Bigelow Laboratory for Ocean Sciences and 84:04 from the Maine Benthic Research Group. We wish to thank M. Bender and several anonymous reviewers for many helpful suggestions.

REFERENCES

- Anonymous. 1979 NLIN Procedure. in SAS User's Guide 1979 Edition. J. T. Helwig and K. A. Council, eds. SAS Institute Inc., NC, USA. 494 pp.
- Armstrong, P. B., W. B. Lyons and H. E. Gaudette. 1979. Application of formaldoxime colorimetric method for the determination of manganese in the pore water of anoxic estuarine sediments. *Estuaries*, 2, 198–201.
- Bender, M. L., K. A. Fanning, P. N. Froelich, G. Ross Heath and V. Maynard. 1977. Interstitial nitrate profiles and oxidation of sedimentary organic matter in the eastern equatorial Atlantic. *Science*, 198, 605–609.
- Billen, G. 1976. Evaluation of nitrifying activity in sediments by dark ^{14}C -bicarbonate incorporation. *Water Res.*, 10, 51–57.
- Christensen, J. P. 1983. Electron transport system activity and oxygen consumption in marine sediments. *Deep-Sea Res.*, 30, 183–194.
- Deuser, W. G., E. H. Ross and R. F. Anderson. 1981. Seasonality in the supply of sediment to the deep Sargasso Sea and implications for the rapid transfer of matter to the deep ocean. *Deep-Sea Res.*, 28A, 495–505.

- Devol, A. H. 1978. Bacterial oxygen uptake kinetics as related to biological processes in oxygen deficient zones of the oceans. *Deep-Sea Res.*, 25, 137-146.
- Ericson, D. B., M. Ewing, G. Wollin and B. C. Heezen. 1961. Atlantic deep-sea sediment cores. *Geol. Soc. Am. Bull.*, 72, 193-285.
- Emerson, S., R. Jahnke, M. Bender, P. Froelich, G. Klinkhammer, C. Bowser and G. Setlock. 1980. Early diagenesis in sediments from the eastern equatorial Pacific. I. Pore water nutrient and carbonate results. *Earth Planet. Sci. Lett.* 49, 57-80.
- Froelich, P. N., G. P. Klinkhammer, M. L. Bender, N. A. Luedtke, G. R. Heath, D. Cullen, P. Dauphin, D. Hammond, B. Hartmann and V. Maynard. 1979. Early oxidation of organic matter in pelagic sediments of the eastern equatorial Atlantic: suboxic diagenesis. *Geochim. Cosmochim. Acta*, 43, 1075-1090.
- Gardner, W. S., D. S. Wynne and W. M. Dunstan. 1976. Simplified procedure for the manual analysis of nitrate in seawater. *Mar. Chem.*, 4, 393-396.
- Goloway, F. and M. Bender. 1982. Diagenetic models of interstitial nitrate profiles in deep sea suboxic sediments. *Limnol. Oceanogr.*, 27, 624-638.
- Grundmanis, V. and J. W. Murray. 1982. Aerobic respiration of pelagic marine sediments. *Geochim. Cosmochim. Acta*, 46, 1101-1120.
- Gundersen, K. and C. W. Mountain. 1973. Oxygen utilization and pH change in the ocean resulting from biological nitrate formation. *Deep-Sea Res.*, 20, 1083-1091.
- Hinga, K. R., J. McN. Sieburth and G. Ross Heath. 1979. The supply and use of organic material at the deep-sea floor. *J. Mar. Res.*, 37, 557-579.
- Jahnke, R. A., S. R. Emerson and J. W. Murray. 1982. A model of oxygen reduction, denitrification, and organic matter mineralization in marine sediments. *Limnol. Oceanogr.*, 27, 610-623.
- Jenkins, M. C. and W. M. Kemp. 1984. The coupling of nitrification and denitrification in two estuarine sediments. *Limnol. Oceanogr.*, 29, 609-619.
- Jorgensen, B. B. 1977. Bacterial sulfate reduction within reduced microniches of oxidized marine sediments. *Mar. Biol.*, 41, 7-17.
- Richards, F. A. 1965. Anoxic basins and fjords, in *Chemical Oceanography*, 1, J. P. Riley and G. Skirrow, eds., Academic Press. New York, 611-645.
- Rowe, G. T. 1981. The deep-sea ecosystem, in *Analysis of Marine Ecosystems*, A. R. Longhurst, ed., Academic Press. New York, 235-267.
- Rowe, G. T. and C. H. Clifford. 1978. Sediment data from short cores taken in the northwest Atlantic Ocean. W.H.O.I. Technical Report 78-46. 55 pp (Unpublished manuscript).
- Rowe, G. T. and W. D. Gardner. 1979. Sedimentation rates in the slope water of the northwest Atlantic Ocean measured directly with sediment traps. *J. Mar. Res.*, 37, 581-600.
- Sayles, F. L. 1981. The composition and diagenesis of interstitial solutions-II. Fluxes and diagenesis at the water-sediment interface in the high latitude North and South Atlantic. *Geochim. Cosmo Chim. Acta*, 45, 1061-1086.
- Seitzinger, S. P., S. W. Nixon and M. E. Q. Pilson. 1984. Denitrification and nitrous oxide production in a coastal marine ecosystem. *Limnol. Oceanogr.*, 29, 73-83.
- Smith, K. L. Jr. 1978. Benthic community respiration in the N.W. Atlantic: *in situ* measurements from 40-5200 meters. *Mar. Biol.*, 47, 337-347.
- Smith, K. L. Jr., G. A. White, M. B. Laver and J. A. Haugsness. 1978. Nutrient exchange and oxygen consumption by deep-sea benthic communities: preliminary *in situ* measurements. *Limnol. Oceanogr.*, 23, 997-1005.
- Sorensen, J., D. J. Hydes and T. R. S. Wilson. 1984. Denitrification in a deep-sea sediment core from the eastern equatorial Atlantic. *Limnol. Oceanogr.* 29, 653-657.

- Strickland, J. D. H. and T. R. Parsons. 1972. A practical handbook of seawater analysis, 2nd edition. Fish. Res. Bd. Canada, Bull. 167, 1-310.
- Vanderborght, J. P. and G. Billen, 1975. Vertical distribution of nitrate concentration in interstitial water of marine sediments with nitrification and denitrification. *Limnol. Oceanogr.*, 20, 953-961.
- Wilson, T. R. S. 1978. Evidence for denitrification in aerobic pelagic sediments. *Nature* 274, 354-356.